Linear Driving Force Approximation to a Radial Diffusive Model

Hakan Başağaoğlu and Timothy R. Ginn
Dept. of Civil and Environmental Engineering

Benjamin J. McCoy
Dept. of Chemical Engineering and Materials Science

Miguel A. Mariño
Dept. of Land, Air and Water Resources, and Dept. of Civil and Environmental Engineering
University of California, Davis, CA 95616

Transient volume-averaged and spatial intraparticle contaminant concentration in a dissolved phase of spherical immobile aggregates is examined using the linear driving force (LDF) model, a special case of a generalized concentration profile (GCP) approximation. Particular cases are solved when a mass flux occurs between the surrounding bulk concentration and intraparticle concentration. Four different forms for the time-variant surrounding bulk concentration are considered: linear, exponential, sinusoidal (oscillatory) and step function. Both pointwise and volume-averaged intraparticle concentrations computed by the LDF model match the numerical and analytical (when available) solutions almost perfectly, when the surrounding bulk concentration is assumed to be changing linearly or exponentially. For the other two cases, however, only volume-averaged concentrations across the immobile spherical particle and the temporal concentrations at the outer boundary of the particle computed from the LDF approximation match the numerical model results reasonably well.

Introduction

A radial diffusion model has commonly been used in various disciplines to simulate the rate-limited mass-transfer processes of contaminants in porous media, for example, in soil-water, soil-vapor, and sediment-water systems (Wu and Gschwend, 1986; Gierke et al., 1990, 1992; Haggerty and Gorelick, 1995; Ng and Mei, 1996) in gas-particulate systems in the atmosphere (Rounds and Pankow, 1990), and sorptive kinetics of persistent persticide residues in seawater (Gonzalez-Davila et al., 1995). The radial diffusion model has also been used for the fixed-bed adsorber to model intraparticle diffusion rates (Rasmuson and Neretnieks, 1980; Tomida and McCoy, 1987; Li and Yang, 1999) and for the simulated moving bed to describe intraparticle mass-transfer rates in bi-disperse porous adsorbents (Azevedo and Rodrigues, 1999).

Because the LDF approximation, which goes back to Glueckauf (1955), provides substantial simplifications in computations, it has been widely employed in various problems that involve intraparticle diffusion (Rice, 1982; Goto et al., 1990; Farooq and Ruthven, 1991; Peker et al., 1992; Rodrigues and Dias, 1998; Li and Yang, 1999). Liaw et al. (1979) showed that the LDF method of Glueckauf (1955) for a particle mass transfer could be approximated by a parabolic concentration profile for intraparticle diffusion (Rice et al., 1983; Do and Rice, 1986). The GCP approximation to the intraparticle concentration reduces the transient radial diffusion model with complex boundary conditions to a first-order simple ordinary differential equation for both the intraparticle volume-averaged and the point-wise contaminant concentration across the soil aggregates.

Assuming no external mass-transfer resistance, Li and Yang (1999) utilized the radial diffusion model to determine the diffusion of adsorbate within an adsorbent particle. They considered a symmetry condition at the center and a specified time-variant concentration profile (Dirichlet boundary

Correspondence concerning this article should be addressed to H. Başağaoğlu.

condition) at the outer boundary of an immobile spherical particle. In this article, their radial diffusion model will be modified by replacing the Dirichlet boundary condition by a more general Robin boundary condition to account for the mass transfer between the immobile phase within the particle and the surrounding bulk concentration. The radial diffusion model will then be solved for four different scenarios in which surrounding bulk concentration varies in time: (1) linear; (2) exponential; (3) oscillatory; and (4) step function. To analyze the performance of the LDF approximation, analytical (when available) and numerical solutions for the four cases will be compared with the intraparticle concentration profiles that will be derived through the LDF and GCP approximations.

Radial Diffusion Model

The sorptive interaction between surface sediments, colloidal particles, and persistent contaminant residues strongly affects the transport and fate of contaminant residues in surface and subsurface water. One of the most common models to simulate the rate-limited mass transfer between the immobile zone within a spherical particle (sediment, soil, particulate, and so on) and the surrounding bulk concentration is the radial diffusion model (Wu and Gschwend, 1986)

$$\frac{\partial S_r}{\partial t} = \frac{\beta D_m}{r^2}\frac{\partial}{\partial r}\left(r^2\frac{\partial C_r}{\partial r}\right) \tag{1}$$

in which S_r is the total local volumetric concentration in the porous sorbent (M/L^3), C_r is the intraparticle contaminant concentration in a dissolved phase (M/L^3), β is the porosity of the sorbent, D_m is the pore fluid diffusivity of the sorbate (L^2/T), and r is the radial distance from the center of a spherical grain. When the sorption process is linear and reversible, Eq. 1 can be rewritten in terms of the dissolved concentration (Ng and Mei, 1996)

$$\frac{\partial C_r}{\partial t} = \frac{D_e}{r^2}\frac{\partial}{\partial r}\left(r^2\frac{\partial C_r}{\partial r}\right) \tag{2}$$

$$D_e = \frac{\beta D_m}{(1-\beta)\rho_s K_p + \beta} f(\beta, t) \tag{3}$$

in which D_e is the sorption-retarded effective intraparticle diffusivity (L^2/T), K_p is the equilibrium partition coefficient (L^3/M), ρ_s is the bulk density (M/L^3), and $f(\beta, t)$ is a correction factor for the diffusion coefficient (Wu and Gschwend, 1986) that includes the effects of tortuosity and intra-aggregate porosity [$f(\beta, t)$ is taken unity in this article].

The initial and boundary conditions for the intraparticle contaminant concentration in a dissolved phase can be expressed as

$$C_r(r,0) = C_0 \tag{4}$$

$$\frac{\partial C_r(r,t)}{\partial r} = 0 \qquad \text{at} \quad r = 0 \tag{5}$$

$$D_e\frac{\partial C_r(r,t)}{\partial r} = k_f\left[C_{\text{bulk}}(t) - C_r(R,t)\right] \quad \text{at} \quad r = R \tag{6}$$

in which C_0 is the initial intraparticle concentration that remains constant across the spherical solid particle (M/L^3), $C_{\text{bulk}}(t)$ is the surrounding bulk concentration in a dissolved phase (M/L^3), k_f is the mass-transfer coefficient (L/T), and R is the radius of the immobile spherical particle (L). An analytical solution is available for the radial diffusive model given in Eq. 2 with the auxiliary conditions specified in Eqs. 4 through 6 when the surrounding bulk concentration is assumed to vary linearly in time. However, if the surrounding bulk concentration varies as an exponential, oscillatory, or step function, the corresponding analytical solutions would likely be computationally very intensive, if at all tractable. Thus, only the numerical model will be used to analyze the performance of the GCP approximation and LDF model for those cases.

Volume-Averaged Formulation to Radial Diffusion Model

The volume-averaged concentration of contaminant within the immobile spherical aggregates can be defined as

$$\overline{C}_r(t) = \frac{3}{R^3}\int_0^R C_r(r,t)\,r^2 dr \tag{7}$$

in which $\overline{C}_r(t)$ is the volume-averaged intraparticle concentration within the immobile particles (M/L^3). The volume-averaged equivalence of Eq. 2 can be written using the boundary conditions specified in Eqs. 5 and 6 as follows

$$\frac{\partial \overline{C}_r(t)}{\partial t} = \frac{3k_f}{R}\left[C_{\text{bulk}}(t) - C_r(R,t)\right] \tag{8}$$

Although the volume-averaging reduces the original second-order partial differential equation to a first-order ordinary differential equation, Eq. 8 is intractable unless $C_r(R,t)$ is known beforehand. Difficulties arise in the computation of the volume-averaged concentration, because $C_r(R,t)$ is not necessarily equal to the surrounding bulk concentration when a mass flux between the surrounding bulk and intraparticle concentrations takes place.

Appoximations to Radial Diffusion Model

Generalized concentration profile (GCP) approximation

The intraparticle concentration $C_r(r,t)$ can be represented by the GCP to be a function of two time-dependent parameters $A(t)$ and $B(t)$ and an order of approximation n as in Li and Yang (1999)

$$C_r(r,t) = A(t) + B(t)r^n \tag{9}$$

Liaw et al. (1979) used a parabolic concentration profile ($n = 2$ in Eq. 9) to represent the LDF approximation. Thus, in the subsequent sections, Eq. 9 will be referred to as the LDF model when the order of approximation is equal to 2. When the order of approximation is different from 2, Eq. 9 will be referred to as GCP. The volume-averaged intraparticle concentration and the surrounding bulk concentrations can be written in terms of $A(t)$ and $B(t)$ with Eqs. 6, 7, and 9

as follows

$$\bar{C}_r(t) = A(t) + \frac{3B(t)}{n+3} R^n \tag{10}$$

$$C_{\text{bulk}}(t) = A(t) + B(t) R^n \left(1 + \frac{n}{Bi}\right) \tag{11}$$

$$Bi = \frac{Rk_f}{D_e} \tag{12}$$

in which Bi is the Biot number, or the ratio of external to internal mass-transfer rates. The time-dependent coefficients can be expressed by inversion of Eqs. 10 and 11

$$A(t) = C_{\text{bulk}}(t) - \frac{(n + Bi)(n+3)}{n(n + Bi + 3)} \left[C_{\text{bulk}}(t) - \bar{C}_r(t) \right] \tag{13}$$

$$B(t) = \frac{(n+3)\,Bi}{(n + Bi + 3) n R^n} \left[C_{\text{bulk}}(t) - \bar{C}_r(t) \right] \tag{14}$$

The pointwise intraparticle contaminant concentration in a dimensionless form θ at a distance $\zeta = r/R$ can be calculated in terms of dimensionless surrounding bulk θ_{bulk}, and the volume-averaged intraparticle concentrations $\bar{\theta}$ from Eqs. 9, 13, and 14

$$\theta = \theta_{\text{bulk}} - \frac{(n+3)}{n(n + Bi + 3)} \cdot \left[n + Bi(1 - \zeta^n) \right] \cdot \left(\theta_{\text{bulk}} - \bar{\theta} \right) \tag{15}$$

For a non-zero initial concentration, the following dimensionless concentrations were used in Eq. 15, and will be used in the subsequent sections unless otherwise stated

$$\theta = \frac{C_r(r,t) - C_0}{C_0}; \qquad \bar{\theta} = \frac{\bar{C}_r(t) - C_0}{C_0};$$

$$\theta_{\text{bulk}} = \frac{C_{\text{bulk}}(t) - C_0}{C_0} \tag{16}$$

The volume-averaged intraparticle concentration $\bar{C}_r(t)$ in Eq. 16 can be evaluated from the following ordinary differential equation that can be obtained by first evaluating Eq. 15 at $r = R$, and then substituting the result, expressed in terms of $C_{\text{bulk}}(t) - C_r(r,t)$ into Eq. 8

$$\frac{\partial \bar{C}_r}{\partial t} = \frac{3k_f}{R} \frac{(n+3)}{(n + Bi + 3)} \cdot \left[C_{\text{bulk}}(t) - \bar{C}_r(t) \right] \tag{17}$$

Then, $\bar{C}_r(t)$ from Eq. 17 can be calculated as

$$\bar{C}_r(t) = \bar{C}_r(t=0) \cdot \exp(-\psi t) + \psi \int_{t=0}^{t} C_{\text{bulk}}(t') \exp\left(\psi(t' - t)\right) dt' \tag{18}$$

$$\psi(n) = \xi(n) \cdot \frac{k_f}{R} = \frac{3(n+3)}{(n + Bi + 3)} \cdot \frac{k_f}{R} \tag{19}$$

The integral in Eq. 18 can be evaluated analytically or numerically, based on how the surrounding bulk concentration is defined. Once the volume-averaged intraparticle concentration is calculated from Eq. 18, then the pointwise intraparticle concentration can be calculated directly from Eq. 15. This procedure will be used in comparing the performance of the GCP approximation and the LDF model against numerical and analytical solutions for four different cases in the following sections. The dimensionless form of the volume-averaged intraparticle concentration will be computed and used for all aforementioned cases in the subsequent sections.

Finite Difference (FD) Approximation

As mentioned earlier, an analytical solution is available to the radial dispersion model for a linearly-varying surrounding bulk concentration. For the other cases, however, analytical solutions are not known. In such cases, we resort to numerical solution techniques to examine the performance of the GCP approximation and the LDF model.

The radial diffusion model will be solved using the finite difference approximation based on the Crank-Nicolson scheme with $\alpha = 0.5$ (a weighting parameter between the implicit and explicit finite difference approximations) to ensure that the solution is unconditionally stable. In the FD scheme, it is assumed that there are N nodes and $(N-1)$ intervals with a length of ΔR such that $\Delta R = R/(N-1)$, and with the grid coordinates of $r_i = (i-1)\Delta R$ in which i represents the node number along the radial distance away from the center of particle. The total simulation period is $t_n = n\Delta t$ in which Δt is the time increment and n is the time step index. For $C_i^n = C_i(r_i, t_n)$, the FD approximation for each node can be written as follows:

At the center of the spherical particle $(i = 1)$, $r = 0$ is a singular point for the radial diffusion model. However, the finite difference approximation can still be written using L'Hopital's rule (Özişik, 1989)

$$\tilde{b}_1 C_1^{n+1} + \tilde{c}_1 C_2^{n+1} = \hat{b}_1 C_1^n - \tilde{c}_1 C_2^n \tag{20}$$

in which

$$\tilde{b}_1 = \frac{3D_e}{(\Delta R)^2} + \frac{1}{\Delta t}; \quad \tilde{c}_1 = \frac{-3D_e}{(\Delta R)^2}; \quad \hat{b}_1 = \frac{-3D_e}{(\Delta R)^2} + \frac{1}{\Delta t} \tag{21}$$

For any interior point $(1 < i < N)$

$$\bar{a}_i C_{i-1}^{n+1} + \bar{b}_i C_i^{n+1} + \bar{c}_i C_{i+1}^{n+1} = -\bar{a}_i C_{i-1}^n + b_i C_i^n - \bar{c}_i C_{i+1}^n \tag{22}$$

in which

$$\bar{a}_i = \frac{0.5 D_e}{(\Delta R)^2} \left(\frac{i-2}{i-1} \right); \quad \bar{b}_i = \frac{-D_e}{(\Delta R)^2} - \frac{1}{\Delta t};$$

$$\bar{c}_i = \frac{0.5 D_e}{(\Delta R)^2} \left(\frac{i}{i-1} \right); \quad b_i = \frac{D_e}{(\Delta R)^2} - \frac{1}{\Delta t} \tag{23}$$

At the outer boundary at $r = R$, $(i = N)$

$$a'_N C^{n+1}_{N-1} + b'_N C^{n+1}_N = -a'_N C^n_{N-1} + b'_N C^n_N - \frac{2\Delta R}{D_e} k_f \bar{c}_N \left(C^{n+1}_{\text{bulk}} + C^n_{\text{bulk}} \right) \quad (24)$$

in which

$$a'_N = \left(\bar{a}_N + \bar{c}_N \right); \quad b'_N = \left(\bar{b}_N - \bar{c}_N \frac{2\Delta R}{D_e} k_f \right);$$

$$b''_N = \left(b_N + \bar{c}_N \frac{2\Delta R}{D_e} k_f \right) \quad (25)$$

A set of equations given in Eqs. 20 through 25 was written in tridiagonal matrix form and solved for $C_r(r,t)$ by the Thomas algorithm. After that, the pointwise and volume-averaged concentrations were expressed in terms of dimensionless groups using Eqs. 15 and 16.

Time-Variant Surrounding Bulk Concentration

Li and Yang (1999) considered a specified boundary condition at the outer boundary of the spherical particle without addressing mass-transfer resistance between the surrounding bulk concentration and intraparticle concentration. However, for Dirichlet condition at the outer boundary, $A(t)$, $B(t)$, and $C_r(r,t)$ in Eqs. 1.9 through 1.11 in Li and Yang (1999) should be

$$A(t) = C_r(R,t) - \frac{(n+3)}{n} \left[C_r(R,t) - \bar{C}_r(t) \right] \quad (26)$$

$$B(t) = \frac{(n+3)}{nR^n} \left[C_r(R,t) - \bar{C}_r(t) \right] \quad (27)$$

$$\theta = \theta(\zeta = 1) - \frac{(n+3)}{n} \cdot (1 - \zeta^n) \cdot \left[\theta(\zeta = 1) - \bar{\theta} \right] \quad (28)$$

Following the same procedure outlined in the previous sections, $\bar{C}_r(t)$ can be calculated

$$\bar{C}_r(t) = \bar{C}_r(t=0) \cdot \exp(-\phi t) + \phi \int_{t=0}^{t} C_r(R,t') \exp\left[\phi(t' - t) \right] dt' \quad (29)$$

$$\phi = \phi(n) = \frac{3D(n+3)}{R^2} \quad (30)$$

An algebraic error leading to erroneous conclusion in Li and Yang (1999) was highlighted by Sircar and Hufton (2000). The primary extension of this article beyond Li and Yang's (1999) work is the consideration of mass transfer between the immobile intraparticle concentration within the soil particle and the transient surrounding bulk concentration in the model formulation, through which the performance of the LDF approach is to be tested. This analysis will be performed in the following sections on an immobile spherical grain that has a concentration equal to the surrounding bulk concentration initially ($\bar{C}_r(t=0) = C_{\text{bulk}}(t=0) = C_0$). The bulk concentration will then be varied as a linear, exponential, oscillatory, or step function in time. For each case, the intraparticle concentration will be computed by LDF model and GCP approximation, which will subsequently be compared with the numerical and analytical (when available) solutions.

Case 1: Surrounding bulk concentration varies linearly in time

The surrounding bulk concentration is assumed to vary linearly in time, starting from its initial concentration equal to the uniform initial concentration across the spherical particle [$C_{\text{bulk}}(t) = C_{\text{bulk}}(t=0) + bt$]. The analytical solution for this problem in dimensionless form is (Luikov, 1968)

$$\theta = P_d \cdot \left\{ \tau - \frac{1}{6} \left[\left(1 + \frac{2}{Bi} \right) - \zeta^2 \right] + \sum_{n=1}^{\infty} \frac{A_n}{\mu_n^2} \frac{\text{Sin}(\mu_n \zeta)}{\zeta \mu_n} \exp\left(-\mu_n^2 \tau \right) \right\} \quad (31)$$

in which

$$A_n = (-1)^{n+1} \frac{2Bi \left(\mu_n^2 + (Bi - 1)^2 \right)^{1/2}}{\left(\mu_n^2 + Bi^2 - Bi \right)} \quad (32)$$

$$\tau = \frac{D_e t}{R^2}; \qquad P_d = \frac{bR^2}{D_e C_0} \quad (33)$$

τ is the dimensionless generalized time, which is usually referred to as Fourier criterion (denoted by F_0 in Luikov (1968)), and P_d is the Predvoditelev criteria that characterizes the rate of ambient concentration increase. μ_n in Eq. 32 is determined from the following characteristic equation

$$\tan \mu_n = -\frac{1}{Bi - 1} \mu_n \quad (34)$$

For $\tau \gg 1$, one term is sufficient to evaluate the summation in Eq. 31 adequately (Luikov, 1968). However, for smaller times (as time approaches zero) more terms are needed. In this article, the first six terms were used to compute Eq. 31. Pointwise concentrations for $\tau \geq 0.453$ did not change when more terms in addition to the first two terms are included in evaluating the summation. In contrast, at $\tau = 0$, the uniform nonzero initial concentration C_0 throughout the spherical particle could not be reproduced exactly by using the first six terms alone. The absolute error incurred was in the range of 0.14−1.3%. It should also be noted that $\zeta = 0$ is a singular point to Eq. 31. As in Eq. 20, a solution for Eq. 31 at the center of the particle ($\zeta = 0$) can be obtained using L'Hopital's rule, with an error of 1.8% when only the first six terms are used. The volume-averaged intraparticle solution can also be calculated analytically (Luikov, 1968)

$$\bar{\theta} = P_d \cdot \left\{ \tau - \frac{1}{15} \left(1 + \frac{5}{Bi} \right) + \sum_{n=1}^{\infty} \frac{B_n}{\mu_n^2} \exp\left(-\mu_n^2 \tau \right) \right\} \quad (35)$$

$$B_n = \frac{6\, Bi^2}{\mu_n^2 \left(\mu_n^2 + Bi^2 - Bi \right)} \quad (36)$$

The same problem was solved using the FD and GCP approximations. The convergence analysis was conducted for FD using the analytical solution in Eq. 31 to determine the best spatial and temporal increments in the finite difference formulation. For GCP, the volume-averaged intraparticle concentration in a dimensionless form is computed directly from Eq. 18

$$\bar{\theta} = \frac{P_d}{\xi(n)\cdot Bi}\cdot\left(\xi(n)\cdot Bi\cdot\tau - 1 + \exp\left(-\xi(n)\cdot Bi\cdot\tau\right)\right) \quad (37)$$

Case 2: Transient surrounding bulk concentration that varies exponentially

The surrounding bulk concentration is assumed to be changing exponentially in time, starting from its initial concentration, which is equal to the initial concentration across the spherical particle $[C_{\text{bulk}}(t) = C_{\text{bulk}}(t=0)\cdot\exp(bt)]$. This radial diffusive model was solved using both FD and GCP approximations. The nondimensional, volume-averaged innerparticle contaminant concentration from GCP is

$$\bar{\theta} = \left[\exp\left(-\xi(n)\cdot Bi\cdot\tau\right] - 1 + \psi' \times\left\{\exp\left[\sigma_d\tau + \xi(n)\cdot Bi\cdot\tau\right] - 1\right\}\cdot\exp\left(-\xi(n)\cdot Bi\cdot\tau\right) \quad (38)$$

$$\sigma_d = \frac{bR^2}{D_e}; \qquad \psi' = \frac{\psi}{\psi + b} \quad (39)$$

Case 3: Transient surrounding bulk concentration that displays oscillatory behavior

The surrounding bulk concentration is to display sinusoidal variations in time. The initial bulk concentration is assumed equal to the initial concentration of the spherical particle. The surrounding bulk concentration varies as $C_{\text{bulk}}(t) = C_{\text{bulk}}(t=0)\cdot Cos^2 bt$. As in Case 2, this model was also solved using both FD and GCP approximations. The volume-averaged innerparticle contaminant concentration in dimensionless form for this case is

$$\bar{\theta}(t) = -1 + \left[\left(\frac{\psi}{\psi^2 + 4\lambda^2}\left(\psi\,\text{Cos}\left(\sigma_d\tau\right) + 2\lambda\,\text{Sin}\left(\sigma_d\tau\right)\right)\cdot\exp\left(\xi(n)\cdot Bi\cdot\tau\right)\cdot\text{Cos}\left(\sigma_d\tau\right) + \frac{2\lambda^2}{\psi}\left(\exp\left(\xi(n)\cdot Bi\cdot\tau\right) - 1\right) - \psi\right) + 1\right]\cdot\exp\left(-\xi(n)\cdot Bi\cdot\tau\right) \quad (40)$$

Case 4: Transient surrounding bulk concentration that varies as a step function

Both the particle and the surrounding bulk concentration are assumed to have a zero initial concentration. The concentration of the surrounding media is then incremented to a certain concentration level instantaneously and kept at that level for a certain period $0 < \tau < \tau_0$. At the end of this period $\tau = \tau_0$, the bulk concentration was dropped instantaneously to a level of zero. This model was also solved with the GCP and FD approximations. Different from the aforementioned cases, the dimensionless volume-averaged intraparticle concentration for GCP of Case 4 is obtained by normalizing the concentrations with respect to the maximum bulk concentration ($C_{\text{bulk}-\max}$)

$$\bar{\theta}'(\tau \le \tau_0) = \left[\bar{\theta}'(\tau=0) + \theta'_{\text{bulk}}(\tau=0) \times\left\{\exp\left[\xi(n)\cdot Bi\cdot\tau\right] - 1\right\}\right]\cdot\exp\left[-\xi(n)\cdot Bi\cdot\tau\right] \quad (41)$$

$$\bar{\theta}'(\tau > \tau_0) = \bar{\theta}'(\tau=\tau_0)\cdot\exp\left[-\xi(n)\cdot Bi\cdot\tau\right] \quad (42)$$

in which

$$\bar{\theta}' = \frac{\bar{C}_r(t)}{C_{\text{bulk}-\max}}; \qquad \theta'_{\text{bulk}} = \frac{C_{\text{bulk}}(t)}{C_{\text{bulk}-\max}} \quad (43)$$

Once the volume-averaged intraparticle concentration is calculated, the pointwise concentration across the spherical particle can be calculated directly from Eq. 15 for all cases.

Application

Time-variant pointwise and volume-averaged concentrations over a spherical homogeneous immobile particle surrounded by a spatially-uniform, transient bulk concentration, expressed in various mathematical forms, were analyzed. In these analyses, the Biot number was set equal to 10, consistent with the condition that the Biot number is usually greater than unity for particle mass-transfer processes (Froment and Bischoff, 1979). The parameter b in Case 1, Case 2, and Case 3 that appear in the definition of the surrounding bulk concentrations, were set equal to 2, 0.04, and 1, respectively. Moreover, $P_d = 14.706$, $\sigma_d = 0.882$ (for Case 2), $\sigma_d = 22.059$ (for Case 3) were used in computations. According to convergence analysis on numerical solutions for all cases, the spatial and time domains were discretized into 30 and 4,800 nodal and temporal spacing, respectively.

It is well known from the earlier studies that the LDF approximation may produce a negative concentration profile or significant deviations from the exact profile in short times. For the first case, as an example, negative concentrations were computed by the LDF and GCP approximations when $\tau <$ 0.161. Moreover, the concentration profile computed by the LDF model did not match the exact profile reasonably well for $\tau < 0.360$.

Figure 1 compares the spatial concentrations across the spherical particle computed by the GCP, LDF, analytical and FD models for the first case at $\tau = 0.453$, in which the LDF model matched the analytical and numerical solutions reasonably well. The spatial concentration profiles obtained from GCP approximations, however, diverge from the numerical and analytical model solutions more and more, as we move from the outer boundary towards the inner boundary of the particle. On the other hand, the analytical, FD, and GCP (regardless of "n" chosen for GCP) solutions yielded practically the same concentration level at and near outer boundary of the particle. The same conclusions can also be drawn for case 2 (see Figure 2) in which the performance of the

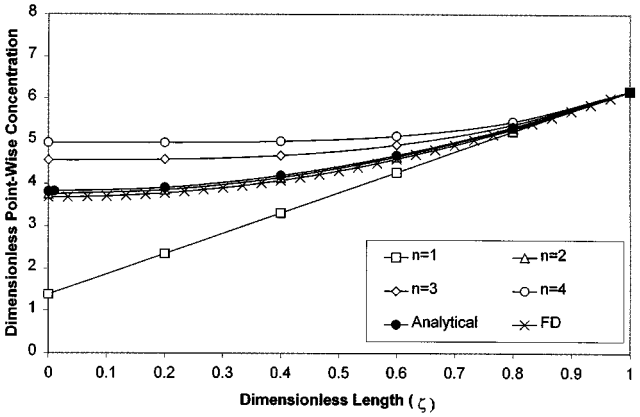

Figure 1. Pointwise concentration across the immobile particle at $\tau = 0.453$ (Case 1).

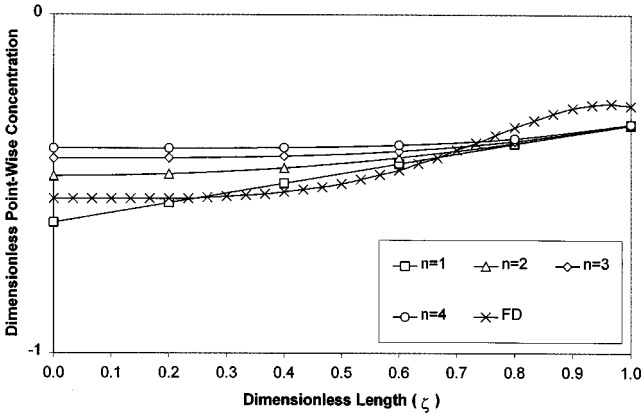

Figure 3a. Pointwise concentration across the immobile particle at $\tau = 0.453$ (Case 3)

GCP and LDF were compared with solutions from the FD model alone. The same pattern in Figures 1 and 2 was also observed at later times, for example, at $\tau = 0.907$ and $\tau = 2.267$, although they are not included in this article.

Figure 3a shows the spatial concentration profiles for case 3 at $\tau = 0.453$, obtained from the FD model compared with GCP approximations. Unlike the first two cases, neither the GCP nor the LDF model could match the concentration profile computed by the FD model across the particle reasonably well. However, LDF solution apparently followed the numerical solution slightly better than GCP approximations. At $\zeta = 1$, both the LDF model and the GCP approximations agreed with the solution from the FD model reasonably well. The same conclusion was also found valid for concentration profiles at later times (they are not shown in this article). Figure 3b shows, that, although the FD and the LDF models produced totally different spatial concentration profiles at the inner boundary, as well as across the particle at three distinct times, the computed point concentrations at the outer boundary of the particle from those two models approached to the same concentration level at each time.

For case 4, concentration profiles obtained from the GCP with a lower order of approximations, specifically $n = 1$ and $n = 2$, conformed to the solution obtained from the FD model slightly better. At and near the outer boundary of the particle, concentration profiles obtained from the FD, LDF, and GCP with various orders of approximations converged to the same concentration level (Figure 4), as in case 3. On the other hand, concentration profiles computed by the LDF and GCP displayed significant deviations at and near the inner boundary of the particle, as in the other cases.

Regarding the computed transient volume-averaged concentrations, solutions obtained from the analytical model (only for Case 1), LDF, and GCP (for all cases) were found to be indistinguishable on the curve of the volume-averaged concentration vs. the dimensionless time. Thus, the relative error (absolute percent deviations of LDF and GCP solutions from the analytical solution for Case 1 and from the numerical solution for Case 2) were plotted to show the performance of LDF and GCP approximations (Figures 5 and 6). Dimensionless volume-averaged concentrations were found very small for the third and fourth cases; thus, only deviations from the corresponding numerical solutions were plotted in Figures 7 and 8. In Figures 5 and 6, relatively high error in early

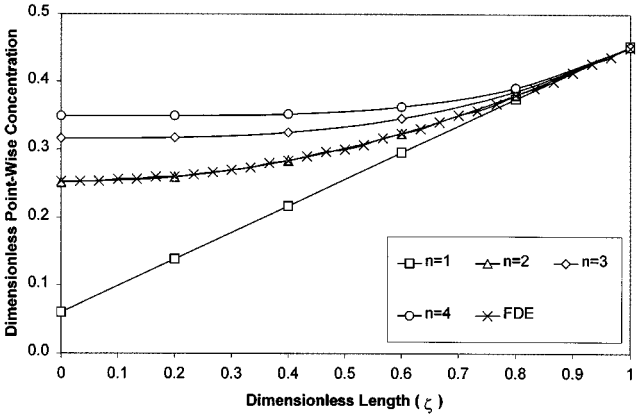

Figure 2. Pointwise concentration across the immobile particle at $\tau = 0.453$ (Case 2).

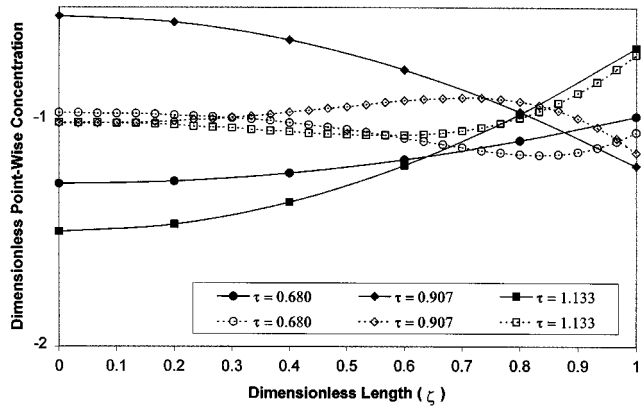

Figure 3b. Pointwise concentration across the immobile particle for Case 3.

Dashed lines correspond to concentrations profiles computed by the FD, whereas solid lines represent the concentrations profiles computed by the LDF.

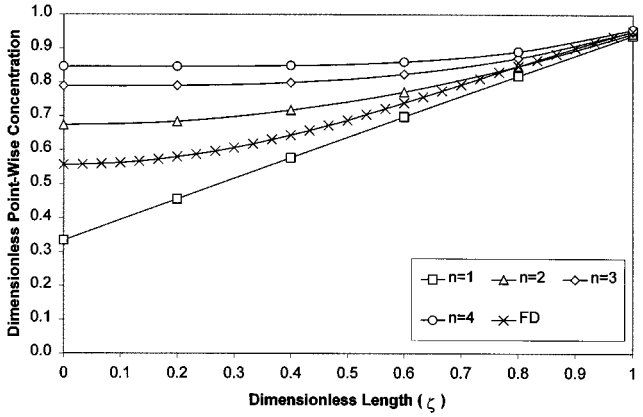

Figure 4. Pointwise concentration across the immobile particle at $\tau = 0.181$ (Case 4).

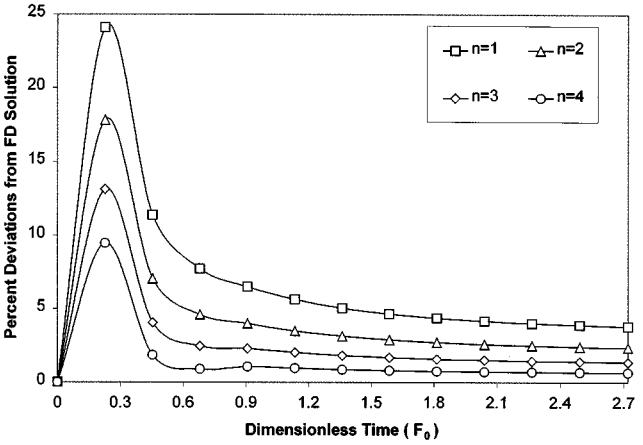

Figure 6. Relative error with respect to the exact solution for Case 2.

times can be attributed to the very small volume-averaged adsorbed amounts during the initial period of the simulation. For the first case, the relative error incurred by the GCP (with $n = 3$ and $n = 4$) and LDF approximations remained below 8% over the entire simulation period. For the second case, the relative error in the LDF model and GCP solutions with ($n = 3$ and $n = 4$), as compared to the numerical solution, was found not exceeding 10% for $\tau > 0.43$. For the third and fourth cases, the LDF solution deviated from the corresponding numerical solution in the range of (-0.11 and 0.06) and (-0.09 and 0.07), respectively. According to Figure 7, the LDF model and GCP solutions (with $n = 1$) displayed practically the same performance for the third case. However, as the order of GCP increases beyond $n = 2$, the maximum discrepancy between the FD and GCP solutions becomes larger. For Case 4, the volume-averaged intraparticle solution obtained from the FD model was approximated better by LDF model and GCP (with $n = 3$ and $n = 4$). As should be expected that as the order of GCP goes up beyond $n = 4$, the range of deviations from the FD model becomes larger.

In light of the above observations, the LDF model can be used to solve the radial diffusive transport model with a general Robin boundary condition, when the surrounding boundary conditions vary monotonously (linearly or exponentially). If the surrounding bulk concentration varies nonmonotonously (oscillatory or step function), then the LDF model can be used if the time-variant volume-averaged concentration values and the time-series of concentration at the outer boundary are of interest.

It is important to note that the pointwise concentrations computed by the LDF and numerical models do not match perfectly for the third and fourth cases, the volume-averaged concentrations and nodal concentrations at the outer boundary match well in all cases. These quantities are important for larger-scale applications, because they characterize the bulk-scale concentrations that matter when accounting upscaled mass balance in multiphase systems. Specifically, the volume-averaged concentrations represent the total mass stored in the intraparticle regimes, and the outer boundary concentrations often determines the mass-transfer rate at the

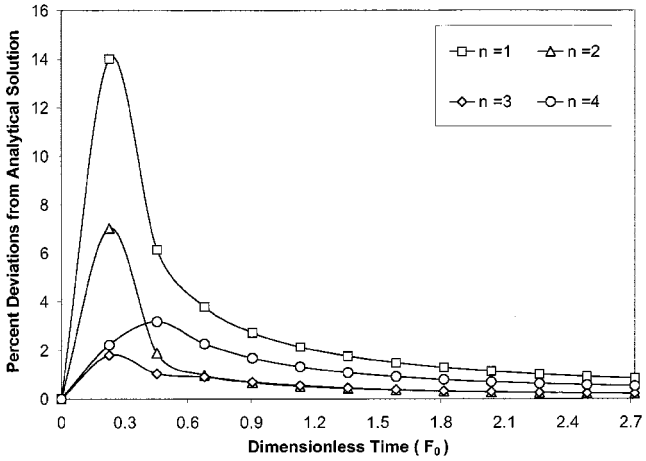

Figure 5. Relative error with respect to the exact solution for Case 1.

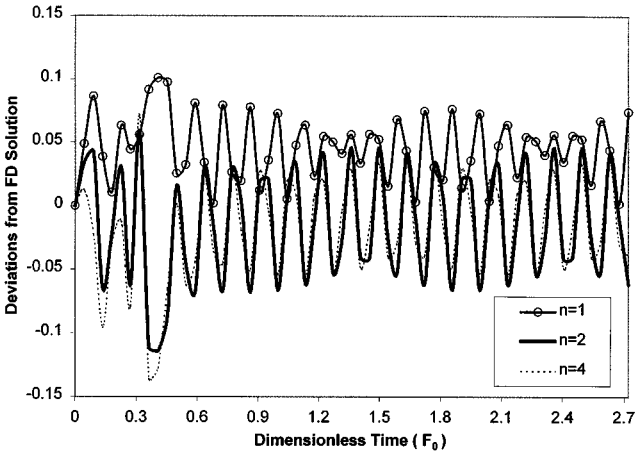

Figure 7. Deviations from the numerical solution for Case 3.

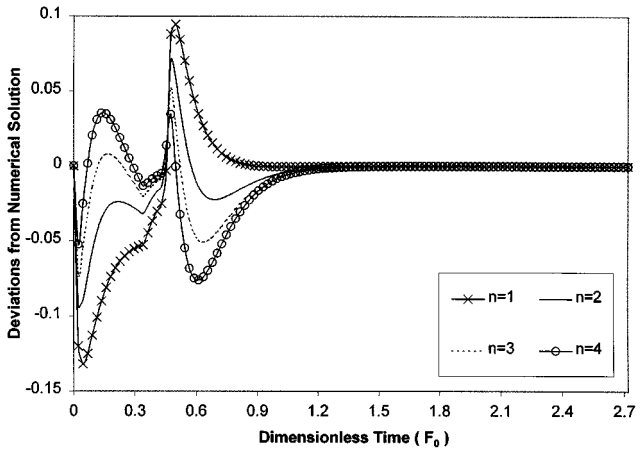

Figure 8. Deviations from the numerical solution for Case 4.

particle-aqueous phase interface in bulk media models, via various nonequilibrium kinetic models. The consistent agreement in simulation of these particular quantities indicates promising potential for the utility of the LDF approach in representing contaminant and other material density fate and transport in field-scale applications that involve the same geometry and coordinates. For instance, mass transfer in saturated porous media occurring in the natural subsurface as well as in packed-bed reactors is often addressed by assuming that the (porous) grains of the porous medium can be treated as identically-sized spheres (Rasmuson and Neretnieks, 1980; Rao et al., 1980, respectively). Mass transfer across the aqueous-solid interface is alternately represented as a first-order kinetic expression (Coats and Smith, 1964; van Genuchten and Wierenga, 1976) involving the difference in concentrations in the aqueous phase and either at the boundary of the particle or volume-averaged within the particle, or, via a diffusive transport within the particle as in Wu and Gschwend (1986), Ball and Roberts (1991), Cunningham et al. (1997), and others including this article. In these latter cases the radial coordinate is intended and used as an effective dimension representing a characteristic length for mass stored within the porous solid phase. A significant contributor to the computational complexity of such models is the diffusion in the radial coordinate. Thus, the simplifications provided by the LDF approach, shown here to consistently respresent the volume-averaged and boundary concentrations, may prove useful in reducing the computational requirements of such field-scale (and reactor-scale) models that involve diffusion along an effective radial coordinate. One of the benefits of the solution described here is that they provide a mechanistic representation of mass transfer that is also more amenable to upscaling than conventional numerical solution.

Conclusions

A radial diffusive transport model that allows a mass exchange between the surrounding bulk concentration and immobile intraparticle concentration was studied to analyze the performance of GCP and LDF models in computing both pointwise and volume-averaged intraparticle concentrations over spherical aggregates. The model was solved for both monotonously and nonmonotonously varying surrounding bulk concentrations. For the particular problem considered in this article, LDF model results agreed fairly well with the pointwise (including both the inner and outer boundary nodes) and volume-averaged intraparticle concentrations computed by analytical (when available) and FD solutions, when the surrounding bulk concentration varied monotonously (linearly and exponentially) in time. However, when the surrounding bulk concentration was assumed to vary nonmonotonously (sinusoidal and step function), only volume-averaged intraparticle concentration and concentration at the outer boundary of the spherical particle computed by the LDF model agreed reasonably well with FD model results.

Acknowledgments

This project was supported in part by the Ecotoxicology Lead Campus Program of the University of California, Toxic Substances Research and Teaching Program. The second author acknowledges support from the U.S. Dept. of Energy's Environmental Science Management Program under the Project entitled ''Dynamics of Coupled Contaminant and Microbial Transport in Heterogeneous Porous Media.''

Literature Cited

Azevedo, D. C. S., and A. E. Rodrigues, ''Bilinear Driving Force Approximation in the Modeling of a Simulated Moving Bed Using Bidisperse Adsorbents,'' *Ind. Eng. Chem. Res.*, **38**, 3519 (1999).

Ball, W. P., and P. V. Roberts, ''Long-term Sorption of Halogenated Organic Chemicals by Aquifer Material, 2, Intraparticle Diffusion,'' *Environ. Sci. and Technol.*, **25**, 1237 (1991).

Coats, K. H., and B. D. Smith, ''Dead-end Pore Volume and Dispersion in Porous Media,'' *J. Soc. Pet. Eng.*, **4**, 73 (1964).

Cunningham, J. A., C. J. Werth, M. Reinhard, and P. V. Roberts, ''Effects of Grain-mass Transfer on the Transport of Volatile Organics through Sediments: 1. Model Development,'' *Water Resour. Res.*, **33**, 2713 (1997).

Do, D. D., and R. G. Rice, ''Validity of the Parabolic Profile Assumption in Adsorption Studies,'' *AIChE J.*, **32**, 149 (1986).

Farooq, S., and D. M. Ruthven, ''Dynamics of Kinetically Controlled Binary Adsorption in a Fixed Bed,'' *AIChE J.*, **37**, 299 (1991).

Froment, G. F., and K. B. Bischoff, *Chemical Reactor Analysis and Design*, Wiley, New York (1979).

Gierke, J. S., N. J. Hutzler, and J. C. Crittenden, ''Modeling the Movement of Volatile Organic Chemicals in Columns of Unsaturated Soil,'' *Water Resour. Res.*, **26**, 1529 (1990).

Gierke, J. S., N. J. Hutzler, and D. B. McKenzie, ''Vapor Transport in Unsaturated Soil Columns: Implications for Vapor Extraction,'' *Water Resour. Res.*, **28**, 323 (1992).

Glueckauf, E., ''Theory of Chromatography: 1. Formula for Diffusion into Spheres and their Applications to Chromatography,'' *Trans. Faraday Soc.*, **51**, 5140 (1955).

Gonzalez-Daviala, M., J. M. Santana-Casiano, and J. Perez-Pena, ''Partitioning of Hydrochlorinated Pesticides to Chitin in Sea Water: Use of a Radial-Diffusion Model to Describe apparent Desorption Hysterisis,'' *Chemosphere*, **30**, 1477 (1995).

Goto, M., J. M. Smith, and B. J. McCoy, ''Parabolic Profile Approximation (Linear Driving Force Model) for Chemical Reactions,'' *Chem. Eng. Sci.*, **45**, 443 (1990).

Haggerty, R., and S. M. Gorelick, ''Multiple-Rate Mass Transfer for Modeling Diffusion and Surface Reactions in Media with Pore-Scale Heterogeneity,'' *Water Resour. Res.*, **31**, 2383 (1995).

Li, Z., and R. T. Yang, ''Concentration Profile for linear Driving Force Model for Diffusion in a Particle,'' *AIChE J.*, **45**, 196 (1999).

Liaw, C. H., J. S. P. Wang, R. H. Greenkorn, and K. C. Chao, ''Kinetics of Fixed-Bed Adsorption: A New Solution,'' *AIChE J.*, **25**, 376 (1979).

Luikov, A. V., *Analytical Heat Diffusion Theory*, Academic Press, New York (1968).

Miller, C. T., and W. J. Weber, ''Sorption of Hydrophobic Organic Pollutants in Saturated Soil Systems,'' *J. Contam. Hydrol.*, **1**, 243 (1986).
Ng, C-O., and C. C. Mei, ''Aggregate Diffusion Model Applied to Soil Vapor Extraction in Unidirectional and Radial Flows,'' *Water Resour. Res.*, **32**, 1289 (1996).
Özişik, N., *Boundary Value Problems of Heat Conduction*, Dover, New York (1989).
Peker, H., M. P. Srinivasan, J. M. Smith, and B. J. McCoy, ''Caffeine Extraction Rates from Coffee Beans with Supercritical Carbon Dioxide,'' *AIChE J.*, **38**, 761 (1992).
Rao, P. S. C., D. E. Rolston, R. E. Jessup, and J. M. Davidson, ''Solute Transport in Aggregated Porous Media: Theoretical and Experimental Evaluation,'' *Soil Sci. Soc. Am. J.*, **44**, 1139 (1980).
Rasmuson, A., and I. Neretnieks, ''Exact Solution of a Model for Diffusion in Particles and Longitudinal Dispersion in Packed Beds,'' *AIChE J.*, **26**, 686 (1980).
Rice, R. G., ''Approximate Solutions for Batch, Packed-Tube and Radial-Flow Adsorbers—Comparison with Experiment,'' *Chem. Eng. Sci.*, **37**, 83 (1982).
Rice, R. G., K. C. Nadler, and F. C. Knopf, ''Comparison of Exact and Approximate Solutions of Transient Response for Leaching by SCF in CSTR,'' *Chem. Eng. Comm.*, **21**, 55 (1983).
Rodrigues, A. E., and M. M. Dias, ''Linear Driving Force Approximation in Cyclic Adsorption Process: Simple Results from System Dynamics Based on Frequency Response Analysis,'' *Chem. Eng. Process*, **37**, 489 (1998).
Rounds, S. A., and J. F. Pankow, ''Applications of a Radial Diffusion Model to Describe Gas/Particle Sorption Kinetics,'' *Environ. Sci. and Technol.*, **24**, 1378 (1990).
Sircar, S., and J. R. Hufton, ''Interparticle Adsorbate Concentration Profile for Linear Driving Force Model,'' *AIChE J.*, **46**, 659 (2000).
Tomida, T., and B. J. McCoy, ''Polynomial Profile Approximation for Intraparticle Diffusion,'' *AIChE J.*, **33**, 1908 (1987).
van Genuchten, M. T., and P. J. Wierenga, ''Mass Transfer Studies in Sorbing Porous Media, 1, Analytical Solutions,'' *Soil Sci. Soc. Am. J.*, **40**, 473 (1976).
Wu, S. C., and P. M. Gschwend, ''Sorption Kinetics of Hydrophobic Organic Compounds to Natural Sediments and Soil,'' *Environ. Sci. and Technol.*, **20**, 717 (1986).

Manuscript received Nov. 15, 1999, and revision received Apr. 27, 2000.